Current Clinical and Medical Education

Received 30 Jun 2024 | Revised 29 Jul 2024 | Accepted 20 Aug 2024 | Published Online 6 Sep 2024

Published By: Vision Publisher

CCME 02 (9), 53-69

ISSN 2942-0792

Magnetic Resonance Spectroscopy: MRI Scanner, Cerebral Proton Spectroscopy, and Using of PET/CT Scanning in Cancer Patients

Aiham Sajjad Abed[1], Ali Saeed Mousa[2], Mohammed Jabbar Hasan[3]

[1,2,3]Al-Hillah University College, Department of Medical Devices Engineering Technology, Iraq

Abstract:

The elimination of the need for patients to undergo potentially harmful ionising radiation exposure is one of the many ways in which the advent of magnetic resonance imaging (MRI) has revolutionised medical research and diagnosis. The utilisation of magnetic resonance imaging (MRI) is expanding in clinical practice due to its increasing availability and lowering cost. In order to make more informed therapeutic decisions, it is helpful to have a firm grasp of the concepts underpinning this imaging modality and its various uses. Reviewing the fundamentals of magnetic resonance imaging (MRI), this article goes on to cover its many clinical uses, including parallel, diffusion-weighted, and magnetisation transfer imaging. A review of important metabolites and their potential interpretation is also provided, along with an examination of MR spectroscopy. The price of magnetic resonance imaging (MRI) scanners has already dropped significantly, making them more accessible. However, experts predict that this trend will only accelerate in the years to come. Magnetic resonance cholepancreatography (MR chole) and magnetic resonance imaging (MRI) of the brain, pancreas, liver, and abdomen will be standard procedures. The widespread deployment of 3 T machines, which are already in use in some locations, is likely to lead to an even stronger magnetic field. Magnetic resonance imaging (MRI) will become increasingly important in routine diagnosis as a result of improvements in resolution and tissue contrast, leading to a decline in the use of invasive diagnostic techniques like endoscopy. In conclusion, we believe that the doctor would benefit greatly from understanding the fundamental physics principles of magnetic resonance imaging (MRI). To make sure the methods are used appropriately, it is important to know their limitations. The notion of nuclear "spin" and the reaction of nuclei to external magnetic fields form the basis of the working mechanism of MRI. To create a free-induction decay and, by extension, a signal that can be transformed into interpretable data, magnetic resonance (MR) pulses need to be supplied at the resonant frequency of a particle. To pinpoint MR signals in space or tissue, MR gradients are necessary. These are created by strategically placing several radiofrequency coils in various locations throughout the room. In order to shorten the scan duration, parallel imaging makes use of several RF coils. T systems have a better signal-to-noise ratio and more resolution than the standard 1.5 T models used in clinical practice, making them ideal for use in research settings. To indirectly assess protein/lipid components relative to body water, magnetisation transfer imaging can be employed to see typically MR-invisible protons attached to macromolecules. The water component of the brain can be imaged using diffusion-weighted imaging, and water flow can be studied in great detail at the microscopic cellular level using diffusion tensor imaging. Using chemical shift imaging or singlevoxel spectroscopy, Magnetic Resonance Spectroscopy may ascertain the precise chemical composition of a specimen.

Keywords : MRI Scanner, Cerebral Proton Spectroscopy, PET/CT Scanning, Cancer patients.

Corresponding Author: Aiham Sajjad Abed†, Al-Hillah University College, Department of Medical Devices Engineering Technology, Iraq

Introduction

It was for their 1946 experimental descriptions of the nuclear magnetic resonance (NMR) phenomena that Bloch and Purcell were jointly given the Nobel Prise for Physics in 1952. Since then, thanks to the advent of wide-bore superconducting magnets (around 30 years ago), the method has undergone fast evolution, enabling the development of clinical applications. Today, magnetic resonance imaging (MRI) is a strong and extensively used clinical technology; the first clinical MRIs were created in 1980 in Aberdeen and Nottingham. This article begins with a quick review of MRI's foundational ideas then moves on to a discussion of the technology's present medical applications. The protons and neutrons that make up an atomic nucleus always have a positive net charge. The number of protons determines a feature called "spin" in certain atomic nuclei. For example, the hydrogen nucleus (1 H) and the phosphorus nucleus (31 P) both have spin. Although it is a mathematical analogy, one way to think about it is as the nucleus spinning on its own axis. Even though it doesn't spin in the traditional sense, the nucleus induces a magnetic moment in its constituent parts, creating a local magnetic field with north and south poles. Similar to classical mechanics of spinning objects, this dipolar magnet can be described quantum mechanically. Like a bar magnet, the dipole has two magnetic poles that line up along its axis of rotation. The nucleus can be aligned parallel to or perpendicular to an external, strong magnetic field (B0). When a solution with numerous nuclear spins is placed in the B0 field, those spins will be in one of two energy states: either a low-energy state, which is perpendicular to the direction of the magnetic field, or a high-energy state, which is parallel to the field. A preponderance of spins perpendicular to B0 is expected in solids and liquids. The nucleus will precess about the B0 axis because it has an angular momentum from its revolution, even if a bar magnet would be oriented perfectly parallel or antiparallel to the field. The use of the word "spin" to describe what is actually a quantum mechanical event is based on this behaviour, which is likened to the swaying of a gyroscope in response to the Earth's magnetic field. The Larmor frequency is the rotational velocity with respect to the field direction. This is defined by the Larmor equation and is directly proportional to the field strength. Inside the static magnetic field B0, spin-containing nuclei can be stimulated by means of a second radiofrequency (RF) magnetic field B1, which is applied in a direction perpendicular to B0. Pulses of microseconds in duration are typical for applying RF radiation. As the nucleus absorbs energy, its energy levels drop, and when it relaxes, they rise again. A voltage is produced by the nuclei's absorption and subsequent emission of energy; this voltage can be detected by a wire coil that is appropriately tuned, amplified, and shown as the "free-induction decay" (FID). When the RF pulse stops, the system will go back to its original temperature state thanks to relaxation mechanisms. Thus, when subjected to the same magnetic field, each nucleus will exhibit a unique resonance frequency. A change in energy level can be induced by measuring the energy gap between two nuclear spin states. The intensity of the B0 magnetic field that the nuclei are exposed to determines this. To create a FID, an RF pulse is applied at the resonant frequency. In actuality, the signal-to-noise ratio (SNR) is enhanced by averaging the results of numerous FIDs obtained by applying RF pulses in succession. An FID that is averaged across time is a signal in the time domain. It will include nuclear components from a variety of sources in the investigated environment, such as free water and 1 H bound to tissue, among others. Using a mathematical procedure called Fourier transformation, the signal-averaged FID can be converted into a frequency spectrum that provides biochemical information or an image (MRI).

RF COILS with MR Field Gradients

Through the use of gradients, the MR signal can be spatially localised to an area of interest. The static field strength varies in several additional spatially linear ways. The MR system's three sets of gradient coils—Gx, Gy, and Gz—allow for the application of gradients in any orthogonal direction. The MR signal is either stronger or lower when the precession rate is faster or slower. Therefore, it is possible to reconstruct images in three dimensions by using the frequency measurements to differentiate MR signals at various spatial locations. Depending on the part of the body being studied and the type of experiment, the transmitter and receiver coils could be two distinct pieces of gear. An enveloping transmitter coil, like a head coil, applies the B1 pulse uniformly around the region of interest. A loop of wire, known as the receiver coil, can be integrated into the transmitter coil or positioned immediately above the area of

interest. Multiple coils in a phased-array configuration receive an MR signal from a single source of stimulation at the same time. You can achieve a better signal-to-noise ratio by connecting each coil to its own receiver; this is because the noise from the coils is not correlated with each other. After that, we may use mathematical methods to merge the data from each coil and get the best possible reconstructed image.

Imaging in Parallel

To cut down on scan times, MR imaging employs parallel imaging. For instance, there is sensitivity encoding (SENSETM, Philips) and SMASH, which stands for simultaneous acquisition of spatial harmonics. SENSE is able to function by simultaneously gathering data from numerous imaging coils and under-sampling the MR data. Accurate knowledge of the individual coil sensitivities prior to data capture is required for data reconstruction. Hence, before the main imaging sequence, a reference scan is obtained with low resolution individual coil data. A decrease in the amount of MR signal that is recorded may occur, however, with larger SENSE factors.

Using an MRI Machine

Cryogenic superconducting magnets with strengths between 0.5 and 1.5 Tesla (T) are used by modern diagnostic MRI scanners. The Earth's magnetic field, on the other hand, is 0.5 Gauss (G), or 0.00005 T. It is usual practice to immerse the magnet in liquid helium to bring its temperature near to zero Kelvin (K), which enables the conduction of such massive currents. The majority of clinical studies were performed at a 1.5 T field strength up until very recently. The capabilities of 3 T systems are being optimised and investigated in the research setting, where they are already widely employed and widely available. A higher signal-to-noise ratio (SNR), better quantification, and increased spatial, temporal, and spectral resolution are all benefits of systems with a stronger field of view. A shorter imaging duration is possible in exchange for the improved SNR. Constructive flaws consist of magnetic sensitivity, eddy current anomalies, and magnetic field instability [4-6]. A material's or tissue's magnetic susceptibility is the degree of magnetisation when subjected to a magnetic field. Depending on your perspective, this might improve or degrade the picture quality. Compared to 1.5 T, magnetic susceptibility artefacts are more noticeable at 3 T. Though this phenomena might improve tissue contrasts in functional or diffusion MRI, it would be problematic in diffusion sequences because it would create signal holes at the interfaces between air and tissue. The induced current known as an eddy current is created when the MRI scanner's conducting structures interact with the magnet field, which is subject to fast changes. If the gradient field is disturbed by eddy currents, the resulting MR image may have lower resolution.

Weighed T1 and T2 magnetic resonance imaging

After absorbing radiofrequency energy, a nuclear "spin" goes through a process known as relaxation, during which it returns to thermal equilibrium. T1 and T2 are the time constants that characterise the longitudinal and transverse relaxations, respectively.5 The nucleus's immediate surroundings are referred to as the "lattice" in T1, which is another name for the process. Dissipation of energy into the lattice happens during longitudinal relaxation. Time required for the system to return 63% to thermal equilibrium after an RF pulse expressed as an exponential function of time is denoted as T1. Changing the repetition time (TR), the interval between RF pulses, is one way to control T1. Fat looks bright on T1-weighted images due to its short T1 value (260 ms), in contrast to water and cerebrospinal fluid (CSF), which have lengthy T1 values (3000-5000 ms) and look black on these images. It is also possible for a spin system's nuclei to experience energy redistribution during relaxation processes, rather than a loss of energy throughout the system. Consequently, nuclei tend to align mostly along the RF pulse's axis. During relaxation, the nuclei's orientations dephase due to energy transfer, the resultant field direction decreases, and the alignments become more chaotic. This is T2, also known as transverse relaxation, because it quantifies the rate of energy exchange between the spins in the "xy" plane. Relaxation technique 2, or "spin-spin," is another name for T2 [7-9].

The brain's bound and free water compartments can be indirectly measured via magnetisation transfer imaging (MT). Factors such as overall water content, heavy metal concentration, and membrane fluidity can influence it.8,9 MT is a method for adjusting the contrast between different types of tissues.Ten, eleven In addition to facilitating the acquisition of high-contrast pictures, MT-based methods also make it possible to assess MT ratios (MTR). Tissue MR reflectivity (MRR) is a quantitative measure of the behaviour of bound protons to macromolecules that are often not visible to magnetic resonance (MR). Standard magnetic resonance imaging (MR) methods may miss parenchymal

alterations in the brain, but MTR measurement can reveal them.5, Tissue proton concentrations can be broadly divided into two categories: free and bound. The free pool consists of mobile protons like those in human body water; its spectral line is thin and its T1 and T2 relaxation durations are quite long. Since the MR excitation frequency range is somewhat limited and concentrated on these mobile protons, most of the signal in traditional MR applications originates from the free pool. Being MR invisible means that the second pool of protons coupled to proteins or other macromolecules or membranes is not usually within the excitation frequency range that is used. Figure 8 shows that the SNR is lower in this pool because to its shorter relaxation durations and significantly wider spectral line. Bidirectional magnetisation transfer between pools is possible by chemical methods, nuclei transfer, or direct interaction between spins. Under typical conditions, the direction of magnetisation transmission is unaffected.The constrained pool's magnetisation is saturated by five MT techniques, whereas the free pool is largely unaffected. The wide spectral line of the bound pool makes this feasible. An RF pulse applied "off-resonance" can stimulate it. Substantial weakening of the magnetisation results from the bound pool becoming saturated. The free pool experiences a decrease in its effective longitudinal magnetisation and T1 relaxation time due to the minimal transfer of magnetisation. The effect of MT can be measured in various tissues by designing pulse sequences that use "off-resonance" pulses. A narrow spectral line resonating at the Larmor frequency (n0) characterises the free pool of protons (A). To excite the free pool, RF pulses covering the pink-colored frequencies might be used. The blue line represents the frequency offset by Dn, which allows the "bound" pool (B) to be excited and saturated with RF radiation without substantially impacting the free pool.

Imaging Based on Diffusion Weighting

One magnetic resonance imaging (MR) method that can quantify the movement of water molecules is diffusion-weighted imaging (DWI). Acute cerebral ischemia was first detected using DWI in the early 1990s. Examination for brain tumours and multiple sclerosis are two more possible explanations. from eight to ten. Diffusion of water molecules is governed by Brownian motion. Therefore, the motion of water molecules is uniform and random in all directions when not limited. Isotropic motion describes this chaotic motion. The physical constraints of organised settings, however, limit the mobility of water molecules. The cerebral microstructure, which includes both white and grey matter, limits the mobility of water molecules. White matter tracts are best traversed by water molecules in a parallel rather than perpendicular direction. This kind of motion is called "anisotropic" since it does not have a uniform distribution in all directions. Diffusion tensors are mathematical constructs that explain the molecular mobility in three dimensions (x, y, and z) and the correlation between these directions. The characteristics of an ellipsoid in three dimensions are defined by a tensor in mathematics. The diffusion tensor can only be calculated with diffusion data in at least six noncollinear directions. Diffusion tensor imaging describes this procedure. Using DTI, a diffusion map may be generated by calculating the tensor at each pixel position. This map will display the process's magnitude and dominant direction. The paths that are most likely to be followed by diffusion when plotted across multiple pixels are called dominant directions. Tractography is the name given to this method since it is based on the notion that the white matter tracts are represented by the diffusion of these routes.

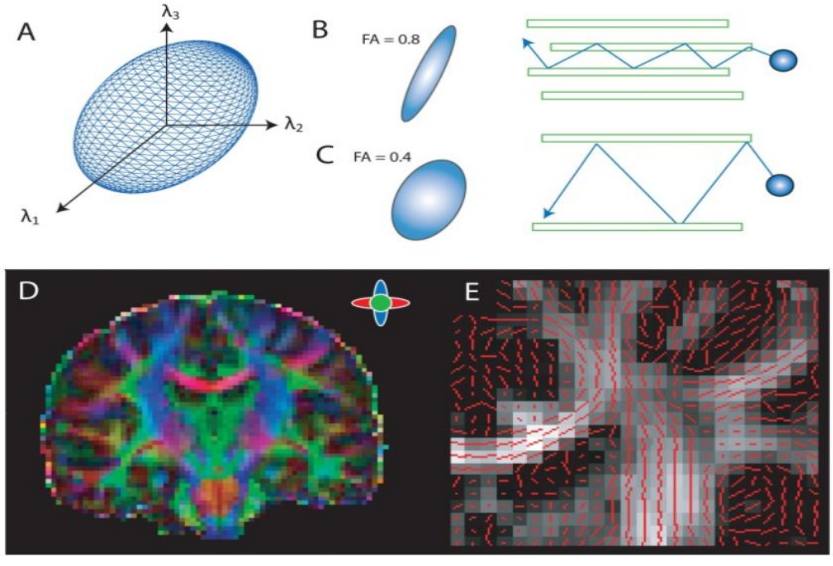

Figure 1. Diffusion principles. (A) As a function of direction, the diffusion tensor ellipsoid shows the likelihood that water molecules in a voxel will diffuse. Using the diffusion tensor, one may determine the fractional anisotropy (FA). A longer extended probability distribution is indicative of areas with strong anisotropy, where one-way diffusion is more likely to occur. (C) A more spherical distribution is observed in areas with lesser anisotropy. (D) Different white matter pathways' major diffusion directions are shown in this coloured FA picture. (E) On top of an FA map (where lighter grey signifies more anisotropy), the red lines depict the primary diffusion directions within each voxel. In white matter, the main diffusion axis often runs parallel to the tract's length.

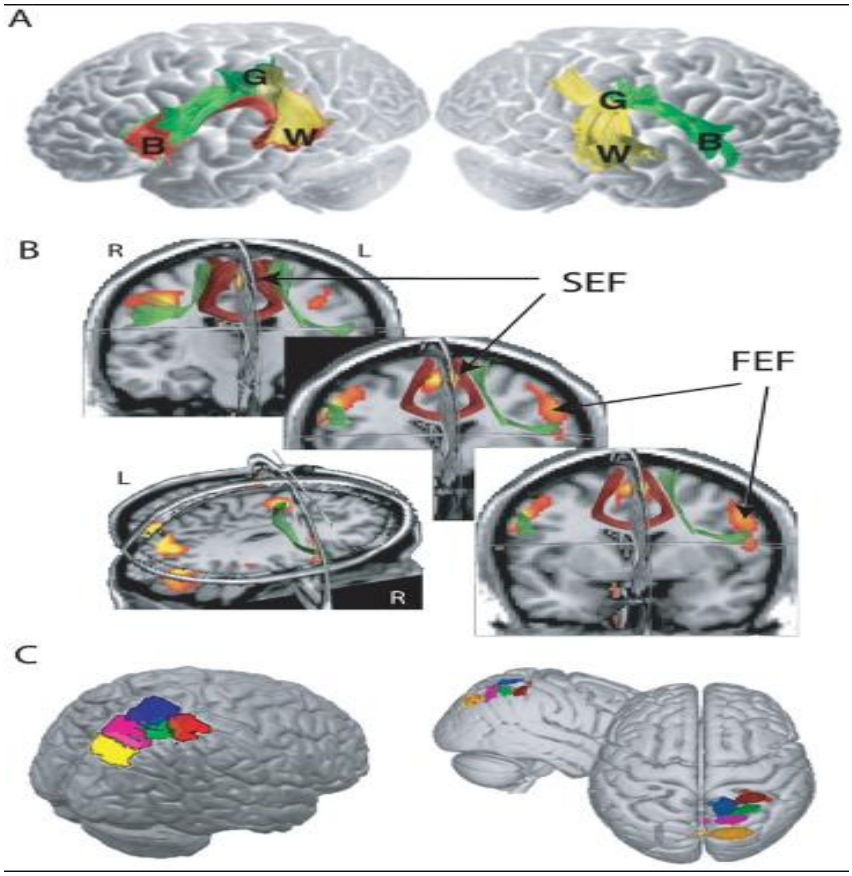

Figure 2. Applications of diffusion tensor tractography. (A) Most subjects showed a remarkable left hemisphere lateralization when pathways connecting Broca region (B), Wernicke area (W), and Geschwind area (G) were considered. Words associated with specific meanings were more easily remembered by those whose right hemisphere Broca-Wernicke circuits were more developed (modified from Catani and others 2007). (B) The results of the group's tractography, which have been normalised and co-registered in MNI space, are superimposed on different slices of the SPM T1 template image (coronal, axial, and sagittal). Additionally, the results of the group's functional magnetic resonance imaging (MRI) are shown, which show the locations of the frontal cortical eye fields (FEF and SEF). Based on the work of Anderson et al. (2011), the green lines represent the links between ipsilateral SEF and FEF, whereas the red lines represent the tract connecting contralateral SEF. (C) The posterior parietal cortex was parcellated using probabilistic tractography, which detects regions of the brain that have similar cortical projections..

Coefficient of Apparent Diffusion (DTI)

Gathers precise data that sheds light on the microstructure present in an imaging voxel. A number of factors are computed, such as the average diffusivity, anisotropy degree, and diffusivity direction. [11–13] Mean diffusivity is a cellular and subcellular level metric for water displacement and the existence of mobility barriers. It is possible to determine the diffusion coefficient by comparing DWI images with varying weights. It is possible to construct an

apparent diffusion coefficient (ADC) image by mapping the several images. The ADC determines the water diffusivity in tissue by observing the interactions between water molecules and their chemical and structural surroundings.

The Isotropy of Fractions

There are a few common ways to express the amount of anisotropy: fractional anisotropy (FA) and relative anisotropy (RA). There are a number of physical factors that influence isotropy, including the size, shape, orientation, density, and direction of nerve fibres inside white matter tracts. There is evidence that myelination is not required for anisotropy to occur, but it does play a role in its development; nonmyelinated nerves can also display anisotropy. One way to visualise the anisotropy and the fibres is with color-coded two-dimensional maps. Another option is to use three-dimensional tractography. By utilising eigenvectors and eigenvalues, a number of techniques can be applied to determine the orientation of the primary axonal fibre bundles. The most recent advancements in this technology, the three-dimensional representation of DTI data, may shed light on the causes of connection failures in the brain.

Magnet Resonance Power

In diffusion-weighted imaging, there are benefits to using 3 T field strength for clinical imaging rather than 1.5 T. The benefits include a signal-to-noise ratio that is 30-50% better, a contrast-to-noise ratio that is up to 96% better, and a variability in ADC and FA that is 34-52% lower. The drawbacks of imaging at 3 T include susceptibility artefact and image distortion, but these can be greatly reduced using parallel imaging techniques like SENSETM (sensitivity encoding). The values of FA and ADC that are obtained should not be affected by field strength, but the accuracy and precision of those measurements should be enhanced [14-16].

Differing Diffusion Paths

Since the body's cellular structures are not uniformly oriented in a perfectly symmetrical alignment, the directionality of the water molecules' diffusion can be measured with some degree of uncertainty. To get a rotationally invariant estimate of isotropic diffusion, it is necessary to measure diffusion in many directions. To find the minimum number of diffusion directions needed to get an isotropic voxel, which can then be used to derive robust ADC and FA data, allowing for a reasonable scan time for the patient while still acquiring valid data, several modelling methodologies and experiments have been conducted. even though there is a minimum need of 6 noncollinear directions for ADC calculations. The properties of the magnetic resonance (MR) sequence determine the diffusion weighting, which is represented as a b value. As the diffusion weighting grows, the b value also rises; typically, a b value of 1000 s/mm2 is enough for diffusion weighting. To measure brain diffusion, two-point ADC estimates using b0 and 1000 s/mm2 are sufficient .

The use of magnetic resonance imaging

Every MR-sensitive nucleus has a unique magnetic environment. While the B0 and applied B1 fields exert a universal influence on all nuclei, the electrons' magnetic fields in the surrounding chemical substances also exert a local magnetic pull. As a result, the chemical structure determines the precise electronic environment, which in turn determines the extent to which electron currents protect or increase the local magnetic field. The nuclear resonant frequencies will vary depending on the chemical environment. The result is chemical shift, which occurs when nuclei with differing resonance frequencies make up the MR frequency spectrum. The frequency is typically given in dimensionless units (parts per million, ppm) relative to a specified reference point, which is determined by the exact magnetic field strength; in 1 H MR spectroscopy, this is typically water at 4.7 ppm. If suitable coils are available to address the issue of poor signal-to-noise ratio in these isotopes, clinical MRS investigations can also be conducted on 13C, 23Na, and 19F in addition to the major nuclei studied, 1H and 31P. A resonance is another name for a peak in an MR spectrum. There may be two (or more) distinct peaks for certain metabolites. The metabolite concentration is given by the region beneath the peak. Metabolite absolute quantification is theoretically conceivable but in practice can be challenging due to considerations such as T1 and T2 effects.

Information Gathering

Chemical shift imaging and single-voxel spectroscopy are the two primary clinical methods for in vivo magnetic resonance spectroscopy. An organ's single-voxel spectra can be defined using gradients in single-voxel spectroscopy. The user specifies the voxel size in advance, and it is the sole signal generator. Scanning for longer periods of time may be necessary to obtain more signal averages in order to enhance the signal-to-noise ratio in smaller voxels. Chemical shift imaging (CSI) uses a voxel matrix to get spectra. Although it is theoretically possible to do this in all three directions, the moniker "2D-single slice CSI" comes from the fact that it is often done in just one plane. The signal-to-noise ratio is higher with single-voxel spectroscopy, but CSI covers more ground anatomically .

Spectroscopy with a Single Voxel

Spectroscopy sequence, echo time (TE), metabolite concentration, and peak height are all factors in MRS. To minimise signal attenuation caused by T1 relaxation and T2 decay, the ideal TR is 2000 ms, preferably 1500 ms, and the TE is as short as possible, typically 30-35 ms. The TE dictates the information gathered; a short TE maximises data acquisition, while a longer TE reduces signal attenuation caused by unwanted macromolecule resonances [18-20], like lipids.

Sequences of MRS

There are a variety of MRS sequences available, each with its own unique pulse sequence and localisation technique. In the past, the only sequence that could achieve low echo times was stimulated echo acquisition mode (STEAM). One 90-degree pulse and two 180-degree pulses make up point-resolved spectroscopy (PRESS). Only protons inside the voxel will get all three RF pulses since each pulse contains a slice selective gradient on one of the three main axes. When compared to STEAM, the signal intensity obtained with PRESS is two times higher. These days, short-echo-time PRESS can be made using modern machinery and procedures.

Analysing Data

When trying to make sense of MRS data, there are a number of factors to think about. Data accuracy is influenced by various experimental factors, including hardware (coil characteristics, receiver linearity, field homogeneity, and voxel homogeneity), water suppression efficiency, voxel localisation by pulse sequence, and the analysis technique technique used to quantify the data. The analytic method and the physical properties of the tissues being studied are additional factors to think about. varied types of brain tissue, such grey and white matter, have varied water concentrations, for instance. Consequently, if the tissue composition of a voxel cannot be precisely established, calculations of metabolite concentrations may be impacted when water is utilised as an internal reference for quantification. There is a possibility of variability in the metabolite ratios when spectra are analysed by various investigators because there are numerous software programmes available for analysing MRS data.42 For example, the results for metabolite levels can change when spectra that are identical are analysed using different approaches.

Electron microscopy of the brain reveals metabolic byproducts

Cerebrospinal fluid MR spectra typically show the following peaks: N-acetyl aspartate (NAA), choline, creatine, myo-inositol, and the combined glutamine and glutamate peak (Glx). Lactate may also be observed. The following concentrations were measured at a time interval of 30 ms: 2.0 ppm for the NAA resonance, 3.2 ppm for cho, 3.0 ppm for Cr, 3.6 ppm for mI, 2.1–2.5 ppm for the Glx complex, and 1.3 ppm for the lactate doublet. Although its precise physiological function is unknown, the main peak observed on water-suppressed proton spectroscopy is N-acetyl aspartate.42 This compound is clinically utilised to monitor the course of multiple sclerosis and is considered a sign of neural dysfunction and neuronal death. Since the release of phosphocholines occurs during membrane breakdown, choline is thought of as a sign of membrane activity. Phosphocholines have an important role in glial cell osmotic control and phospholipid metabolism. Inflammatory and cancerous processes are associated with an enhanced choline resonance, which may indicate gliosis, membrane deterioration from myelin breakdown, and increased cellularity [21–23]. Hepatic encephalopathy has been linked to osmoregulatory alterations, including decreased choline resonance. The combined peak of creatine and phosphocreatine is known as creatine, and it is commonly used as an internal standard. Its concentration in healthy and sick brains is thought to stay constant. A sugar alcohol called myo-inositol is involved in the production of phosphoinositides and in the regulation of cerebral osmolyte levels; elevated myo-inositol levels have been linked to the activation of microglia and astrogliosis; and there is a relationship between

glutamine and glutamate metabolism. In some disease states, like HIV-related dementia, creatine levels may be affected. Astrocytes use glutamine synthetase to convert glutamate and ammonia into glutamine after they have been taken up from the capillaries. After then, glutaminase converts glutamine to glutamate, a neurotransmitter, which neurones then absorb.

Measurement of Metabolites

The concentration of metabolites in MRS can be expressed in two basic ways: as absolute values or as ratios. Absolute quantification can be achieved by using either external reference solutions, or tissue water, as an internal reference in the MR scanner. The benefit of absolute quantification is that it can describe concentrations of individual metabolites and how they vary in disease states. But there are other methodological and technical problems. The inhomogeneity of the B1 field un the two separate zones of interest is a cause for worry when using external reference solutions. It is necessary to assume the water content when using water as an internal reference; however, this might change in disease states and focused lesions. differing types of brain tissue, such as grey and white matter, may also contain differing amounts of water. Because water makes up more than 70% of brain tissue mass, its concentration in the brain is more than 10,000 times higher than that of most metabolites (10 mmol/L). Consequently, the determined metabolite concentrations will be impacted by even little inaccuracies in the absolute water concentration's value assignment. Since extra measurements need to be obtained while a patient is in the MR scanner and the effects of T1 and T2 relaxation on water and metabolite peaks must be considered with absolute quantification methods, the examination time is prolonged. Metabolite ratios are based on the potentially flawed assumption that creatine concentrations remain constant throughout health and illness. Since both comparisons take place at the same instant and in the same area of interest, the error should be dynamic and, thus, smaller.

Analysis of MRS

In most cases, proprietary software is used to integrate or line-fit the Fourier converted signal in order to determine the metabolic peaks. One software package that incorporates the prior knowledge methodology is JMRUI, which uses the AMARES algorithm. This approach can improve accuracy and is defined as previously obtained information regarding the component characteristics of the spectrum. It is likely that different hardware and acquisition sequences will have different impacts on this information. Reduced user-dependent input, which can cause further operator-dependent variability, is another benefit of using past knowledge. JMRUI performs time-domain spectra analysis. The time domain is preferable to the frequency domain for spectroscopic data analysis because it allows for better handling of artefacts like baseline roll and any underlying broad spectral

Cancer patients undergoing PET/CT scans: theoretical and methodological issues

In the field of oncologic positron emission tomography (PET), the current emphasis is on the practical and technological uses of a relatively new technique: the PET/CT scanner, which combines the capabilities of PET and CT scanners into one. By comparing a PET scan with a separate CT scan, PET/CT improves upon the prior state-of-the-art approach and contributes to patient care. Examples highlight this point. Last but not least, the author summarises some of the newly published findings from PET/CT imaging investigations [31–33]. Peptid emission tomography (PET) is a well-established nuclear imaging technique that has been particularly helpful in the field of oncology, nearly 30 years after its inception. The Mallinckrodt Institute of Radiology at Washington University in the mid-1970s developed PET, and it quickly became an invaluable research tool in the fields of cardiology and neurology. It took researchers almost ten years to figure out that PET could be useful in cancer treatment as well. Creating the radiopharmaceuticals utilised for PET imaging necessitates not only a PET scanner that costs over a million dollars, but also costly equipment and highly skilled workers. But thousands of these scanners are already operational all across the globe. Imaging techniques like PET capture biochemical or physiologic events, as opposed to the intricate anatomy shown by CT or MRI. This is why PET provides significant benefits in oncologic imaging compared to anatomic imaging modalities. In cases where CT and MRI fail to differentiate between benign and malignant lesions, PET is frequently able to do so. The positron-emitting radionuclides are attached to tiny, biologically significant molecules—such as sugars, amino acids, nucleic acids, receptor-binding ligands, water, and molecular oxygen—in order to create PET images. The sites of these positronemitting tracers can be detected by the PET scanner when they decay radioactively. To generate "physiologic maps" of the relevant activities or processes, we can image the temporal

distribution of these labelled substances. While there are many PET imaging tracers available, 18F-2-fluoro-2-deoxy-D-glucose (FDG) is currently used in the great majority of clinical oncologic PET scans. An fact that was initially reported 75 years ago—that malignant cells have higher rates of aerobic glycolysis than normal tissues—is used to visualise glucose metabolic rate using FDG. As a result, the cancer cell increases its glucose consumption to fulfil its energy demands. Despite the fact that there are numerous other ways in which cancer cells differ from healthy tissues (such as receptor levels, nucleic acid uptake and incorporation rates, amino acid uptake and incorporation rates, and a plethora of other biologic features that could be assessed with PET), the Food and Drug Administration (FDA) has only authorised FDG as an agent for oncology studies at this time. Thankfully, while FDG isn't a foolproof imaging agent (some tumours have low avidity for FDG and certain benign processes have high avidity), it works wonderfully for the majority of clinically significant malignant tumours (prostate cancer being the biggest exception). Similar to glucose, FDG is taken up by the same membrane transporters and phosphorylated by the same hexokinases [34-36]. In a standard clinical oncology research, patients are given FDG intravenously while they are at rest and then given another 60 to 90 minutes to circulate before imaging can begin. On the next PET scan pictures, areas of hypermetabolism, or "hot spots," will depict the locations of active tumours in the majority of malignant neoplasms. Table 1 displays the indications for PET that have been approved by Medicare. The majority of people seeking cancer diagnosis and treatment fall within these criteria. Notable omissions include certain tumour types for which FDG-PET has shown less efficacy or for which CMS finds inadequate evidence to warrant including the rather costly test in the workup. There are certain tumour types where PET cannot be used. While positron emission tomography (PET) can be useful for assessing the extent of breast cancer, it is not a reliable method for making a first diagnosis. First, the tumour must be of follicular origin, ruling out medullary tumours. Second, the patient must have undergone thyroidectomy and radioiodine ablation before PET scanning can be considered. Third, there must be suspicion of recurrence based on an elevated thyroglobulin level. Lastly, the results of the whole-body iodine study must be negative. These are the very specific criteria set by CMS for PET scanning in patients with thyroid cancer. While PET imaging is now authorised for use in cervical cancer initial staging, restaging with PET is still pending approval [37–39]. In addition, in late 2005, CMS will begin providing coverage for a wider range of tumours; however, this will only be applicable to patients who participate in clinical trials or who enrol in a PET tumour registry that is still in the works. Reimbursement policies for PET studies vary among other payers. Use of PET should be treated with caution for certain tumour types, as the outcomes have been rather varied. These tumours include hepatocellular carcinoma, cholangiocarcinoma, and several sarcomas. Overall poor FDG absorption can be caused by a low overall glucose metabolic rate, low levels of Glut-1 and other transporters, or high amounts of glucose-6-phosphatase, which can be observed in some tumours. Out of all the major tumours for which FDG-PET has typically been ineffective, prostate cancer has the highest incidence and has the most impact on the population. There is a need for more research into the use of tracers other than FDG, but preliminary results have been promising with some of these tumours that do not contain FDG.

Tools and Methods for PET

PET imaging differs from other nuclear medicine imaging techniques in that it is "coincidence" imaging. In order to capture PET images, a patient is encircled by a series of rings made of specialised detector crystals. A positron, an electron with a positive charge, is produced in every decay event. While passing through tissue, this positron usually doesn't reach more than a few millimetres before having a "annihilation reaction" with an electron. In this process, the two particles turn their mass into energy, which is mainly released as two 511 keV photons moving in opposite directions. The PET scanner records and pinpoints the event as a positron annihilation (or "event") because it detects all of the photons at once (or "in coincidence"). By amassing millions of these events, state-of-the-art PET devices can reconstruct images of the tracer's distribution using complex software and hardware. Detector rings containing thousands of individual detector crystal elements around the patient in most PET scanners used since the early 1990s. These scanners may simultaneously produce up to 47 transaxial "slices" across an approximately 14 to 15 cm swath of the body. Scan the normal patient using a "step-and-shoot" method, which involves seven or eight bed-steps, from the bottom of the head all the way up to the proximal femurs, an area where the majority of metastatic illness is most likely to be located. A rotating, three-dimensional, maximum-intensity-pixel "projection" image is frequently helpful for a global view of this massive quantity of data, and the produced images comprise hundreds of sagittal, transaxial, coronal, and MRI-like images. Compared to other imaging modalities, such as CT and MRI, typical PET produces far

lower-resolution pictures, and the imaging technique is notoriously bad at defining anatomical detail. Lesions are not well-localized, and their borders are not clearly defined, due to this lack of information. In addition, lesions are frequently multi-faceted, with certain areas exhibiting higher metabolic activity compared to others. Thus, biopsy or targeted radiation frequently need improved localisation. To overcome this limitation, improve picture interpretation, and ultimately deliver a more precise diagnosis, two modalities are being integrated into a PET/CT scanner.

So, why is PET/CT being used?

For more than 20 years, CT has been the gold standard in oncologic imaging. However, CT cannot detect important physiological changes. PET's unparalleled capacity to ascertain tissue metabolic activity is hindered by the fact that it does not possess the requisite higher-resolution anatomical data. When combining PET with other tomographic modalities, CT is the most straightforward and detailed option. To increase diagnosis accuracy and localisation of numerous lesions, the two can be combined to form an integrated data set that delivers the best of both worlds. For a long time, visual fusion—where a specialist looked at the individual PET and CT scans and mentally synthesised the data—was the main way to combine the metabolic and anatomical information. These days, lots of people are trying software fusion, which involves aligning and "fusing" two sets of data using specialised software. On the other hand, there are a lot of issues with these software approaches. For example, the patient's position might change between the studies, there are differences in breath-hold at maximal inspiration for CT and PET imaging, and the tables on the two devices might have different contours. Integrating the two units into a single gantry was the initial big step towards resolving this issue, proposed in 2000 by the team led by imaging physicist Dr. David Townsend of the University of Pittsburgh. Because of this, the PET and CT data sets can be collected in rapid succession with little room for error in the registration process. These days, PET/CT scanners are made by a number of the big names in imaging equipment. A small number of PET-only scanners are currently available in the US market, as the focus of PET equipment has moved significantly towards PET/CT in recent years. Figure 3 displays the North Texas Clinical PET Institute's state-of-the-art PET/CT scanner, which was installed at the Baylor Sammons Cancer Centre in early 2004. The "tunnel" of a PET/CT device is wider in diameter than that of an MRI scanner, and it is deeper than a CT scanner or a regular PET scanner, albeit it is not quite as deep as an MRI scanner. With a smaller gantry and a larger bore to alleviate claustrophobia, the makers of these scanners have significantly increased patient acceptance in the brief time they have been available for purchase. However, this may not solve the problem entirely, and premedication may still be necessary for those with claustrophobia. Modern, multislice spiral CT scanners are located near the front of the gantry for the great majority of devices on the market today. A cutting-edge PET scanner is the brains behind this. Even a seemingly insignificant problem, like making sure that both scanners use the same table position registration to ensure that the images align correctly, can be a challenge when combining these two machines. Following are the steps of the PET/CT scanning procedure [40-42]. After the FDG injection, the patient is positioned supine on the imaging table sixty to ninety minutes later. A topogram, or digital x-ray of the whole field of interest, is then produced by using the CT tube and detector in the same way as a diagnostic CT. The topogram is utilised to identify the exact area of the body that has to be scanned, and the system is then given those coordinates. The table is then automatically realigned by the scanner software, and a spiral CT scan of the target area (often the area from the base of the skull to the mid-thigh for most cancer studies) is taken, producing hundreds of transaxial images all over the body. The table then moves backwards to the PET scanner section of the machine, which starts the "emission" portion of the PET scan by detecting the patient's radiation emissions. "Stepping" the patient through the scanner produces 30–45 consecutive transaxial images, takes 2–5 minutes per bed-step, and photographs a swath of 14–15 cm through the patient. It usually takes around 30 minutes to complete the scanning process for an oncology study. Scanning the complete body becomes more time-consuming when it's needed, like in the case of melanoma sufferers. There is a vast amount of data produced. It all starts with reconstructing hundreds of transaxial CT and PET scans. To make image interpretation easier, these are rearranged into sagittal and coronal formats. "Fusion" images that combine PET and CT data are also created for each of these sets of images. This means that 4,000 to 8,000 images can be produced by an oncologic PET/CT scan on average. The interpreters' workloads and the resources available for data archiving and retrieval are both strained by this .

Problems with PET and PET/CT Data Interpretation

It can be difficult to draw conclusions from PET tests due to several variables. The most common ones that arise in everyday practice include: unusual tumour sites, limited resolution of small lesions, altered biodistribution of FDG due to hyperglycemia or hyperinsulinemia, bone marrow activation, motion artefacts, and variable physiologic uptake of FDG by normal tissues. Infections and inflammations can also affect FDG uptake. When determining whether to order a PET study and when interpreting the clinical importance of the PET results, both the referring physician and the interpreting physician should keep these potential traps in mind. Only glucose uptake can be measured with FDG-PET. Not only do non-cancerous cells ingest glucose, but so do most cells in the body. Some normally functioning tissues can exhibit extremely variable physiological uptake. Some animals' reception of FDG is unpredictable, while others accumulate it to a predictable degree. As an example, since the brain exclusively metabolises glucose, it usually displays significant absorption of FDG. In contrast, myocardial uptake is intense in people who have not fasted but very variable in those who have. The uptake of FDG by adipose tissue is usually quite low, but in patients who are anxious or chilly, specific adipose deposits (also known as "brown fat") that are involved in thermogenesis can be greatly stimulated. Premedication with benzodiazepines and/or beta-blockers can typically minimise this problem. Even routine tasks can occasionally throw you off [43–45]. The proximal tubules of the kidney do not efficiently reabsorb FDG, in contrast to glucose. So, it's safe to assume that the kidneys and bladder will be very active. One possible misunderstanding is that focal pooling of discharged activity in a ureter is the same as hypermetabolic iliac lymph node metastases. Inflammatory or infected locations can occasionally be seen on PET due to the accumulation of FDG by inflammatory cells, particularly macrophages. When evaluating lung lesions or lymph nodes using PET, granulomatous disorders like sarcoidosis, tuberculosis, fungal infections, and Mycobacterium avium-intracellulare infection might pose unique challenges. Significant absorption can occur even in cases of inflammation associated with therapeutic interventions like surgery or radiation. It is generally recommended to wait at least three months after radiotherapy has finished before conducting a PET study, if possible, in order to prevent any potential confusion caused by inflammatory absorption of FDG. In the future, other tracers that have not been approved by the FDA may help clear up some of this confusion. These tracers aim at nucleic acid uptake and other processes that are less common in inflammatory cells. On the other hand, these tracers have their limitations due to their high concentration in regions where FDG is not present. For instance, a nucleic acid analogue will show intense uptake in bone marrow and gastrointestinal mucosa, as well as in malignant cells and other cells that divide quickly. The avidity for FDG is low in some malignant tumours. As indicated before, prostate cancer is one of several cancers that can exhibit low FDG content. Others include bronchoalveolar cell carcinoma, low-grade sarcomas, specific low-grade non-Hodgkin's lymphomas, and even a small number of well-differentiated lung adenocarcinomas. On FDG-PET, the majority of neuroendocrine tumours do not show up very well. The task of tumour detection and staging is usually made more challenging by small lesions or uncommon presentations/locations. PET on its own can't always pinpoint tiny tumours or tell if abnormal FDG uptake is indicative of a tumour or not. As a general rule, PET/CT can help overcome these limitations to some extent, but for insulin-dependent diabetics, the best course of action is for them to eat a small, low-carbohydrate breakfast and take their insulin (or oral hypoglycemic) as prescribed first thing in the morning. About six hours after that, when both the insulin and glucose levels have dropped to a manageable level but have not yet surpassed 150 mg/dL, the FDG injection is supposed to be administered. Patients with cancer who develop glucose intolerance as a side effect of their treatment face a unique challenge. All patients at the North Texas Clinical PET Institute have their blood glucose levels evaluated before receiving FDG. The oncology population faces the significant challenge of bone marrow activation due to the high number of patients undergoing cytokine therapy or experiencing rebounding bone marrow following chemotherapy. Although PET is often highly sensitive for splenic or osseous metastases, cytokine treatment can mask these lesions due to the elevated activity in the bone marrow and spleen. Patients undergoing chemotherapy or suffering from anaemia may exhibit comparable uptake, but to a lesser extent. A standard rule of thumb is to wait at least one week and no more than three weeks after giving short-acting cytokines, long-acting cytokines, or chemotherapy, before doing a PET scan. Motion artefacts are an issue with virtually every imaging modality, although they can be significantly worse with PET/CT imaging compared to regular PET. In order to account for the patient's body's absorption of photons, a "attenuation-correction" scan is acquired for both kinds of scanning. The reconstructed images can be severely compromised if the patient moves between the two sets of data. By circulating a 511-keV photon source around the body and then measuring the attenuation as it passes through the body, a conventional PET scanner can acquire this attenuation scan. To reduce the likelihood of mobility

between the two, this scan happens either just before or just after the emission data is collected at each level of the body that is being scanned. In contrast, attenuation correction is performed by the PET/CT scanner using the CT images that were acquired before the emission data collection began. The PET scanner needs time to "step" through the body, thus there can be a 20- or 30-minute gap between the attenuation scan and the emission scan. There are a lot of chances to move during that time. However, because PET/CT scans often take far less time than regular PET scans, patients may experience less motion owing to discomfort. For these and other reasons, it is important for referring doctors to include relevant clinical details when they ask for a PET scan in oncology patients. This will help the interpreting doctor give the best possible information. Key considerations include: • The type of cancer, when it was diagnosed, and where the lesion was located (even after removal) • Any recent chemotherapy, anaemia, or cytokine treatment • Inflammatory or infectious processes • Radiation therapy, which can cause inflammation • Recent surgery, which can cause linear uptake along the incision • Granulomatous disease • Claustrophobia or anxiety [46-48.[

Positive Aspects of PET/CT

Aside from the overall reduction in scan time, PET/CT offers several significant clinical benefits, such as improved localisation for biopsy or radiotherapy, serendipitous abnormality discovery, confirmation of unusual or abnormal sites, better identification of inflamma tory lesions, and CT visualisation of PET-negative lesions (particularly bone lesions). Examples of these benefits are shown through the use of images from various scenarios. Figure 6 illustrates the practical application of PET/CT in addressing a common issue faced by anxious patients. Although it looks like metastatic adenopathy, the brown fat activity in the supraclavicular area is actually rather normal. Brown fat activates when a patient feels worried or cold because it contains adrenergic receptors and produces heat through glucose metabolism. Brown fat also contains peripheral-type benzodiazepine receptors, therefore if this is observed in a patient, a repeat study with diazepam premedication will often minimise this uptake. There is some preliminary evidence that beta-blockers may reduce brown fat activity as well. Because PET/CT usually only detects activity in adipose tissue and not lymph nodes, it often eliminates the need for a second investigation in these instances. Importantly, PET/CT can localise and characterise abnormal lesions to confirm or rule out cancer. Figure 7 shows a patient with recurrent colon cancer; a CT scan and clinical observations showed that the disease was limited to the liver. The PET scans revealed that the cancer had mostly spread to the liver, with the exception of a little focal area in the face area—clearly an unusual location for colorectal metastases. We didn't need to undertake any additional tests because the PET/CT pictures revealed that the strong activity wasn't from an unusual metastasis but from a persistent periodontal abscess at a root canal site. Better localisation on PET/CT can help with patient treatment even when PET detects a malignant tumour. Figure 8 depicts a patient with a prior diagnosis of colon cancer. Although the precise position of the recurring lesions in the right abdomen is not easily discernible from the PET scans, it is safe to assume that they are either serosal or nodal in nature and may be amenable to excision. The unresectable foci were pinpointed to the right iliacus and psoas muscles by PET/CT. When it comes to tiny lesions or large, partially necrotic masses, PET/CT can also help with biopsy localisation. Where is the patient located? had rectal cancer in the past and was examined again two years following radiation and resection. A presacral mass was detected by diagnostic CT, however a CT-guided biopsy revealed mainly inflammatory and necrotic tissue. The conventional parasacral biopsy technique had gone through regions devoid of substantial quantities of viable tumour, as revealed by the fusion PET/CT pictures. The PET/CT scans led to a second biopsy, which confirmed the presence of a returning tumour. In many cases, the CT appearance and localisation can either rule out or confirm as tumours any questionable foci seen on the PET imaging. Figure 10 depicts a patient undergoing restaging for recurrent breast cancer. Although the focused uptake in the spine on the coronal pictures could be interpreted as a sign of metastasis, the CT imaging revealed that it actually represents inflammation at a location where facet joint arthritis is present. The fusion images revealed that the patient's more intense focus projected within the body of C2, however it seemed to be located in the anterior vertebral body or disc space. A patient was treated on an emergency basis after CT pictures confirmed metastases and nearly total destruction of the lower part of the C2 vertebral body; this prevented the necessity for confirmatory studies, which could have postponed urgent treatment. As indicated earlier, PET isn't always the best choice for tumours because not all of them accumulate FDG well. In these cases, PET/CT can be more helpful. reveals that a patient with low-grade malignancy had extremely low FDG uptake. While PET can clearly show the majority of low-grade non-Hodgkin's lymphomas, it can miss a few. Although the left lung apex lesion can be seen on the PET scan, the destruction of the first and second ribs cannot. Furthermore, a number of cervical spine metastases that are

indistinguishable on PET scans are clearly seen as lytic metastases on CT scans. This is an out-of-the-ordinary instance; in bone lesions, PET usually shows lytic metastases well but blastic metastases poorly. This is because PET imaging requires a large amount of tumour tissue, and lytic lesions usually have such a volume. Because PET has a high "serendipity factor," it can detect cancers that weren't originally suspected when evaluating other types of cancer. During PET scans for lung nodules, for instance, incidental colon carcinomas may be detected. PET/CT scans help characterise these so-called "incidentalomas" better. The PET/CT scans' CT images aren't always the best for diagnosis, but they can reveal other serious problems that don't include FDG, like aortic aneurysms or huge kidney masses. That which is combined. modalities work in tandem to effectively describe surprising or unforeseen tumor-related discoveries. Where is the patient located? patient's low-grade non-Hodgkin's abdominal lymphoma showed moderate to mild FDG uptake. The contrast between CT and PET was striking, making massive adenopathy and small bowel involvement easy to spot. Cervical adenopathy, which was thought to be lymphoma, was also present in the patient. Cervical adenopathy was considerably more hypermetabolic than primary lymphoma, according to the PET scan, indicating a notable biological distinction between the two. In addition, the PET/CT scans identified the main tumour as a comparable hypermetabolic laryngeal lesion. The patient's PET/CT scans revealed a head and neck cancer, ruling out lymphoma as the cause of her cervical adenopathy.

Drawbacks of PET/CT in Comparison to PET PET/CT

offers numerous benefits compared to conventional PET imaging, while it does come with a few drawbacks. To start, some patients experience claustrophobia due to the fact that the PET/CT scanner resembles a tunnel rather than a doughnut. Another important concern is radiation dosimetry. In PET/CT, a full CT scan is conducted, but with different parameters than in a typical diagnostic CT in order to reduce radiation exposure. Depending on the technique used, radiation from a PET/CT scan can often be 5 to 10 times higher than annual background radiation. In general, the radiation from a PET scan is about three to five times as much as a person would receive in one year from naturally occurring "background" radiation exposure from our surroundings and cosmic rays penetrating the atmosphere. Radiation exposure from CT is high, however it is comparable to that from other diagnostic and interventional procedures like fluoroscopy. Radiation exposure from PET/CT scans, for instance, is lower than that of a standard gallium scan and, in some cases, far lower than that of a complex fluoroscopic operation. Because PET/CT scanners use two extremely complex devices instead of one, technical issues are more common in this modality. The whole apparatus can be rendered useless if the PET or CT detectors malfunction. Emission PET images that have undergone CT-based attenuation correction have their potential applications restricted [49,50]. As an example, artefacts in the reconstruction of PET images can be caused by the use of intravenous contrast for CT scans. Why? Because the iodine in intravenous contrast does a far better job of absorbing the lower-energy CT x-rays than the high-energy 511 keV photons used in PET scans. Because of this, the activity level at areas with dense contrast is overestimated during PET image reconstruction because of a "overadjustment" for photon attenuation. This issue should soon be resolved to a large extent with the use of more modern reconstruction methods, together with changes to imaging processes and adjustments to the administration of contrast. It has already been stated that PET/CT can amplify motion artefacts. One particular and crucial aspect of this is the movement of the respiratory system. Due to the patient's respiratory activity during the PET scan, the CT scan should be conducted in a way that aligns with the patient's diaphragm and surrounding organs for the most accurate data registration. For the most accurate CT scans, it is recommended to take the pictures at the very end of tidal breathing, when the diaphragm is in its most relaxed posture (approximately 75% of the time) during normal tidal breathing. Diagnostic CT, on the other hand, is usually done at maximum inspiratory pressure. Researchers analysing these research should not get their hopes up about the PET/CT scans' capacity to pinpoint lesions due to the fact that misregistration does happen. In very unusual circumstances, PET/CT may provide less reliable results than PET alone; this can be because the results are overly dependent on CT data. For instance, despite a higher confidence in the correct readings, a recent study found that PET/CT actually reduced the accuracy of lung cancer staging compared to PET alone. Because PET is often more accurate than CT in these kinds of applications, it's important to handle inconsistencies between the datasets with caution.

Downsides of CT in PET/CT

When it comes to PET/CT, the CT component has some inherent restrictions. As mentioned earlier, CT scans are conducted at lower energy levels to minimise radiation dosimetry. However, this results in images of lesser quality compared to a diagnostic-grade CT scan. Oral contrast is not commonly used, and most studies do not use intravenous contrast augmentation. The North Texas Clinical PET Institute frequently employs diluted oral contrast due to its ability to enhance abdominal CT pictures without compromising PET images. Due to the aforementioned risks, high costs, and potential for imaging artefacts, intravenous contrast is only used in diagnostic CT exams that are specifically requested. Even when used for diagnostic purposes, the PET/CT scanner does have some small restrictions. The biggest one from a clinical standpoint is that the PET/CT scanner's much bigger gantry can't be tilted, unlike a diagnostic CT scanner's gantry, which can be tilted by a few degrees (typically done for special studies of the head and neck to get direct coronal images or to reduce streak artefacts from dental fillings.

Current Clinical Data

The first commercial PET/CT scanners were out in 2002, hence it took until 2004 for a substantial amount of data to start appearing in publications. While some of these studies looked at general populations to see if PET/CT imaging was superior than PET alone, others focused on particular illness types. Patients with a broad range of solid tumours were examined by Antoch et al., with a focus on breast, colon, and lung malignancies. The researchers discovered that PET/CT with integrated hardware improved accuracy slightly. Integrating PET with diagnostic CT increased accuracy by 34% compared to diagnostic CT alone, whereas adding PET to diagnostic CT alone improved staging by 21% (5). Researchers Bar-Shalom et al. observed that combined PET/CT improved image interpretation in 49% of patients and 30% of locations, when they looked at a larger number of patients with mixed kinds of cancer on a per-lesion basis (6). PET/CT altered treatment plans for fourteen percent of patients. Crucially, in cases when the PET/CT altered the study's interpretation, the new interpretation was accurate 95% of the time. Regardless matter how appealing a modern technology may be, it is crucial to check that it is actually improving patient care by delivering better information. When it comes to non-small cell lung cancer, multiple studies have examined the additional benefits of PET and PET/CT for preoperative staging, restaging, and evaluating potential recurrence. These investigations back up what other research has shown over the previous decade: PET has far higher accuracy than CT. When using CT alone, the accuracy was between 63% and 64%, but when using PET alone, the accuracy was between 86% and 90%. When compared to stand-alone PET, the accuracy of integrated PET/CT was just 84% to 93%; however, in 22% to 32% of patients, PET/CT raised the certainty of findings—an important factor in determining the direction and expense of subsequent workup and therapy. The accuracy of PET alone ranged from 74% to 85% in trials involving colorectal cancer patients, while the accuracy of PET/CT was 89% to 97%. In 30–50% of lesions, PET/CT improved the confidence of findings. In their study of 27 lymphoma patients undergoing restaging, Freudenberg et al. examined the findings of several imaging modalities. There was an 84% improvement in accuracy with CT alone, a 95% improvement with PET alone, a 98% improvement with CT and separate PET, and a 99% improvement with hardware-integrated PET/CT. Once again, considering PET's high accuracy in this series whether with or without CT, the main benefit of PET/CT is that it increases the certainty of the diagnosis. The identification of the unidentified primary tumour is a challenging field since no imaging technique has proven useful in localising tumours that have so far evaded traditional evaluation. In a study including 45 patients, Gutzeit et al. determined sensitivity rates of 19% for CT, 28% for PET and CT, 31% for PET and CT combined with hardware integrated PET/CT, and 35% for hardware integrated PET/CT. The respective positive predictive values were 73%, 65%, 81%, and 83%. In the early days of this discipline, some of the published studies used subpar methods, but as time went on, the field improved. The literature on PET/CT is expanding at a rapid pace, the technology is finding new uses in clinical settings, and future research using more effective methods should provide even more promising findings.

CONCLUSION

Innovations in PET/CT technology are intrinsically motivated by the need to better serve patients. Here we shall only mention a handful of those. To start, there will undoubtedly be an ongoing drive for PET and CT components with improved resolutions, which will find their way into future PET/CT machines. How quickly we can get studies of sufficient quality is the second big worry. While PET/CT does reduce the total PET scan time for most patients from 60 minutes to just over 30 minutes, quicker PET scanning is still necessary to enhance scanner throughput and patient comfort. Another development is the creation of organ-specific scanners. For example, there is currently an organ-

specific breast unit available, but its clinical relevance is still uncertain, and it has limited capabilities when it comes to staging the axilla. Combining PET with MRI is another popular idea, but it presents more of a challenge than integrated PET/CT due to issues like the impact of a powerful magnetic field on existing PET detectors and other similar issues. Finally, novel tracers are required to discriminate between malignant tumours and nonmalignant tissues that are FDG-avid, and to aid in the detection of tumours that are not very FDG-avid. For many cancer patients, the imaging standard of treatment for the last decade has been a mix of separate computed tomography (CT) and positron emission tomography (PET). There are a number of significant interpretative and therapeutic benefits to the recent combination of these two scanning modalities into one device. To start with, nonmalignant FDG accumulation sites, including inflammatory foci, brown fat, or muscle uptake, can be more accurately localised to nonmalignant structures, which reduces confusion. Moreover, PET/CT provides enhanced localisation of cancerous lesions, which includes enhanced staging (particularly for extranodal illness), enhanced follow-up of sentinel lesions, enhanced targeting of biopsy and treatment, and higher interpretive confidence. Additionally, PET/CT enhances the identification of tumours that are not FDG-avid, which would otherwise go undetected in a PET investigation. Finally, current research generally shows that overall staging/restaging accuracy improves by 4% to 15% and lesion localisation confidence increases by 30% to 50%. As the method becomes more widely used, these numbers could potentially improve even further.

REFERENCES

1. Lardinois D, Weder W, Hany TF, Kamel EM, Korom S, Seifert B, von Schulthess GK, Steinert HC. Staging of non–small-cell lung cancer with integrated positron-emission tomography and computed tomography. N Engl J Med 2003;348:2500–2507.
2. Antoch G, Saoudi N, Kuehl H, Dahmen G, Mueller SP, Beyer T, Bockisch A, Debatin JF, Freudenberg LS. Accuracy of whole-body dual-modality fluorine-18–2-fluoro-2-deoxy-D-glucose positron emission tomography and computed tomography (FDG-PET/CT) for tumor staging in solid tumors: comparison with CT and PET. J Clin Oncol 2004;22:4357–4368.
3. Bloch F, Hansen WW, Packard ME. Nuclear induction. Phys Rev. 1946;69:127. 2. Purcell EM, Torrey HC, Pound RV. Resonance absorption by nuclear magnetic moments in a solid. Phys Rev. 1946;69:37–38.
4. Hawkes RC, Holland GN, Moore WS, Worthington BS. Nuclear magnetic resonance (NMR) tomography of the brain: a preliminary clinical assessment with demonstration of pathology. J Comput Assist Tomogr. 1980;4(5):577–586.
5. Smith FW, Hutchison JM, Mallard JR, et al. Oesophageal carcinoma demonstrated by whole-body nuclear magnetic resonance imaging. Br Med J (Clin Res Ed). 1981;282(6263):510–512.
6. Westbrook C, Roth CK, Talbot J. MRI in Practice. 4th edition London: John Wiley & Sons, Inc.; 2011. 6. Di Costanzo A, Trojsi F, Tosetti M, et al. High-field proton MRS of human brain. Eur J Radiol. 2003;48(2):146–153.
7. Soher BJ, Dale BM, Merkle EM. A review of MR physics: 3 T versus 1.5 T. Magn Reson Imaging Clin N Am. 2007;15(3):277– 290.
8. Rovira A, Cordoba J, Sanpedro F, Grive E, Rovira-Gols A, Alonso J. Normalization of T2 signal abnormalities in hemispheric white matter with liver transplant. Neurology. 2002;59(3):335– 341.
9. Rovira A, Grive E, Pedraza S, Rovira A, Alonso J. Magnetization transfer ratio values and proton MR spectroscopy of normalappearing cerebral white matter in patients with liver cirrhosis. Am J Neuroradiol. 2001;22(6):1137–1142.
10. Hajnal JV, Baudouin CJ, Oatridge A, Young IR, Bydder GM. Desig and implementation of magnetization transfer pulse sequences for clinical use. J Comput Assist Tomogr. 1992;16(1):7–18.
11. Wolff SD, Balaban RS. Magnetization transfer contrast (MTC) and tissue water proton relaxation in vivo. Magn Reson Med. 1989;10 (1):135–144.
12. Baird AE, Warach S. Magnetic resonance imaging of acute stroke. J Cereb Blood Flow Metab. 1998;18(6):583–609.

13. Moseley ME, Kucharczyk J, Mintorovitch J, et al. Diffusion-weighted MR imaging of acute stroke: correlation with T2 weighted and magnetic susceptibility-enhanced MR imaging in cats. AJNR Am J Neuroradiol. 1990;11(3):423–429.
14. Larsson HB, Thomsen C, Frederiksen J, Stubgaard M, Henriksen O. In vivo magnetic resonance diffusion measurement in the brain of patients with multiple sclerosis. Magn Reson Imaging. 1992;10 (1):7–12.
15. Kono K, Inoue Y, Nakayama K, et al. The role of diffusion-weighted imaging in patients with brain tumors. AJNR Am J Neuroradiol. 2001;22(6):1081–1088.
16. Stadnik TW, Chaskis C, Michotte A, et al. Diffuion-weighted MR imaging of intracerebral masses: comparison with conventional MR imaging and histologic findings. AJNR Am J Neuroradiol. 2001;22(5):969–976.
17. Chenevert TL, Brunberg JA, Pipe JG. Anisotropic diffusion in human white matter: demonstration with MR techniques in vivo. Radiology. 1990;177(2):401–405.
18. Doran M, Hajnal JV, Van Bruggen N, King MD, Young IR, Bydder GM. Norma and abnormal white matter tracts shown by MR imaging using directional diffusion weighted sequences. J Comput Assist Tomogr. 1990;14(6):865–873.
19. Basser PJ, Mattiello J, LeBihan D. MR diffusion tensor spectroscopy and imaging. Biophys J. 1994;66(1):259–267
20. . Basser PJ, Jones DK. Diffusion-tensor MRI: theory, experimental design and data analysis—a technical review. NMR Biomed. 2002;15(7):456–467.
21. Mori S, van Zijl P. 2005, MR tractography using diffusion tensor imaging. In: Gillard J, Waldman A, Barker PB, eds. In: Clinical MR Neuroimaging 1st edition Cambridge University Press; 2005:86– 98.
22. Jones DK. Fundamentals of diffusion MR imaging. In: Gillard J, Waldman A, Barker PB, eds. In: Clinical MR Neuroimaging 1st edition Cambridge University Press; 2005:54–85.
23. Mori S, Barker PB. Diffusion magnetic resonance imaging: its principle and applications. Anat Rec. 1999;257(3):102–109.
24. Le Bihan D, Breton E, Lallemand D, Grenier P, Cabanis E, LavalJeantet M. MR imaging of intravoxel incoherent motions: application to diffusion and perfusion in neurologic disorders. Radiology. 1986;161(2):401–407.
25. Beaulieu C. The basis of anisotropic water diffusion in the nervous system—a technical review. NMR Biomed. 2002;15(7):435–455.
26. Alexander AL, Lee JE, Wu YC, Field AS. Comparison of diffusion tensor imaging measurements at 3.0 T versus 1.5 T with and without parallel imaging. Neuroimaging Clin N Am. 2006;16 (2):299–309.
27. Kuhl CK, Textor J, Gieseke J, et al. Acute and subacute ischemic stroke at high-field-strength (3.0-T) diffusion-weighted MR imaging: intraindividual comparative study. Radiology. 2005;234(2):509– 516.
28. Habermann CR, Gossrau P, Kooijman H, et al. Monitoring of gustatory stimulation of salivary glands by diffusion-weighted MR imaging: comparison of 1.5 T and 3 T. AJNR Am J Neuroradiol. 2007;28(8):1547–1551.
29. Kuhl CK, Gieseke J, von FM, et al. Sensitivity encoding for diffusionweighted MR imaging at 3.0 T: intraindividual comparative study. Radiology. 2005;234(2):517–526.
30. Lee CE, Danielian LE, Thomasson D, Baker EH. Normal regional fractional anisotropy and apparent diffusion coefficient of the brain measured on a 3 T MR scanner. Neuroradiology. 2009;51(1):3–9.
31. Correia MM, Carpenter TA, Williams GB. Looking for the optimal DTI acquisition scheme given a maximum scan time: are more b-values a waste of time? Magn Reson Imaging. 2009;27(2):163–175.
32. Jones DK. The effect of gradient sampling schemes on measures derived from diffusion tensor MRI: a Monte Carlo study. Magn Reson Med. 2004;51(4):807–815.
33. Xing D, Papadakis NG, Huang CL, Lee VM, Carpenter TA, Hall LD. Optimsed diffusion-weighting for measurement of apparent diffusion coefficient (ADC) in human brain. Magn Reson Imaging. 1997;15(7):771–784.

34. Burdette JH, Elster AD, Ricci PE. Calculation of apparent diffusion coefficients (ADCs) in brain using two-point and six-point methods,. J Comput Assist Tomogr. 1998;22(5):792–794.
35. Bottomley PA. The trouble with spectroscopy papers. Radiology. 1991;181(2):344–350.
36. Lundbom J, Hakkarainen A, Fielding B, et al. Characterizing human adipose tissue lipids by long echo time 1 H-MRS in vivo at 1.5 Tesla: validation by gas chromatography. NMR Biomed. 2010;23(5):466– 472.
37. Matthaei D, Frahm J, Haase A, Merboldt KD, Hanicke W. Multipurpose NMR imaging using stimulated echoes. Magn Reson Med. 1986;3(4):554–561.
38. Bottomley PA. Spatial localization in NMR spectroscopy in vivo. Ann N Y Acad Sci. 1987;508:333–348.
39. Klose U. Measurement sequences for single voxel proton MR spectroscopy. Eur J Radiol. 2008;67(2):194–201.
40. Keevil SF, Barbiroli B, Brooks JC, et al. Absolute metabolite quantification by in vivo NMR spectroscopy: II. A multicentre trial of protocols for in vivo localised proton studies of human brain. Magn Reson Imaging. 1998;16(9):1093–1106
41. Bar-Shalom R, Yefremov N, Guralnik L, Gaitini D, Frenkel A, Kuten A, Altman H, Keidar Z, Israel O. Clinical performance of PET/CT in evaluation of cancer: additional value for diagnostic imaging and patient management. J Nucl Med 2003;44:1200–1209.
42. Antoch G, Stattaus J, Nemat AT, Marnitz S, Beyer T, Kuehl H, Bockisch A, Debatin JF, Freudenberg LS. Non-small cell lung cancer: dual-modality PET/CT in preoperative staging. Radiology 2003;229:526–533.
43. Keidar Z, Haim N, Guralnik L, Wollner M, Bar-Shalom R, Ben-Nun A, Israel O. PET/CT using 18F-FDG in suspected lung cancer recurrence: diagnostic value and impact on patient management. J Nucl Med 2004;45: 1640–1646.
44. Cohade C, Osman M, Leal J, Wahl RL. Direct comparison of 18F-FDG PET and PET/CT in patients with colorectal carcinoma. J Nucl Med 2003;44: 1797–1803.
45. Israel O, Mor M, Guralnik L, Hermoni N, Gaitini D, Bar-Shalom R, Keidar Z, Epelbaum R. Is 18F-FDG PET/CT useful for imaging and management of patients with suspected occult recurrence of cancer? J Nucl Med 2004;45: 2045–2051.
46. Even-Sapir E, Parag Y, Lerman H, Gutman M, Levine C, Rabau M, Figer A, Metser U. Detection of recurrence in patients with rectal cancer: PET/CT after abdominoperineal or anterior resection. Radiology 2004;232:815–822.
47. Freudenberg LS, Antoch G, Schutt P, Beyer T, Jentzen W, Muller SP, Gorges R, Nowrousian MR, Bockisch A, Debatin JF. FDG-PET/CT in re-staging of patients with lymphoma. Eur J Nucl Med Mol Imaging 2004;31:325–329.
48. Gutzeit A, Antoch G, Kuhl H, Egelhof T, Fischer M, Hauth E, Goehde S, Bockisch A, Debatin J, Freudenberg L. Unknown primary tumors: detection with dual-modality PET/CT—initial experience. Radiology 2005;234: 227–234